Agent-Based DC Microgrid Control via Digital Twin-Informed Hierarchical Droop

Connor Madden*, Jarrett Peskar*, Kerry Sado†, *Member, IEEE*,
Austin R.J. Downey*‡, *Member, IEEE*, and Jamil Khan*

**Dept. of Mechanical Engineering*
†Dept. of Electrical Engineering
‡Dept. of Civil and Environmental Engineering

University of South Carolina
Columbia, SC 29208 USA
austindowney@sc.edu

***Abstract*—Achieving resilient and efficient power management in naval microgrids requires distributed control of battery energy storage systems (ESS) that account for both electrical and thermal constraints. This work integrates a decentralized adaptive agent-based decision framework with digital twin informed hierarchical droop control. Each agent autonomously manages a battery ESS in a distributed microgrid, leveraging digital twin updated state information to determine load sharing and preserve system health. The system setup uses three ESS to power an auxiliary load within a microgrid. Each ESS consists of a battery and a DC-DC converter supervised by an adaptive agent that uses a digital twin for state estimation. The applied load sequence includes pulsed-load groups at three different rates. This auxiliary load sequence is repeated until one ESS reaches end of life. Simulation results show the hierarchical droop scheme increased system operational lifetime by 23% relative to primary droop with equal load sharing. During simulation testing, all pulsed loads were met, and each battery state of charge converged in 7.2 hrs. The proposed framework suggests a path toward reduced maintenance burden through more balanced battery utilization.**

***Index Terms*—digital-twins, battery modeling, agent-based control, DC microgrids, shipboard energy systems**

I. Introduction

Achieving high efficiency and operational resilience in hybrid microgrids requires energy storage systems (ESS) that can rapidly support load transients while maintaining safe and reliable operation under varying mission profiles. For maritime applications, integration of robust mobile ESS is necessary for smooth shipboard power, necessitating efficient battery management [1]. Often, mission profiles include radar, directed energy weapons, and high-rate pulsed power loads requiring sharp ramping [2]. Meeting rapid load changes can impose damaging electrical and thermal stresses on battery storage, motivating distributed energy storage across the microgrid as a necessary redundancy [3]. Advanced control strategies for hybrid microgrids facilitate efficient battery management, reduced component degradation, and more reliable system performance [4].

Distributed-agent architectures are increasingly employed in microgrids for their cooperative control capabilities and autonomous adaptation to dynamic grid conditions [5]. Prior work presented an adaptive agent-based control scheme to optimize distributed battery implementation into hybrid naval microgrids [6]. The agent-based control scheme links a generator, loads, and distributed battery systems through autonomous, adaptive coordination. The agent's actions where determined with a centralized coordinator. This method improved grid resilience and extended life; however, the centralized coordinator created a single point of failure (SPOF) mode to the system that lacks redundancy necessary for mission critical control. To avoid SPOF, the agents need to operate independently with as few global signals as possible.

Droop control is widely implemented in DC microgrids because it enables reliable load sharing among parallel converters through a fully decentralized approach, allowing each unit to regulate its output using only local measurements, without requiring high-bandwidth communication links [7]. By adjusting output voltage as a function of output current, similar to the behavior of traditional synchronous generators, the converters naturally settle into proportional power sharing based on their droop coefficients. Hierarchical droop control extends basic droop methods by adding secondary and tertiary layers that improve system performance while preserving the decentralized nature of primary droop [8]. Typically, the primary layer provides fast local droop behavior for autonomous load sharing, the secondary layer compensates for voltage deviations and enhances power-sharing accuracy, and the tertiary layer manages higher-level objectives such as optimization across the microgrid, allowing local stability to be maintained while accounting for system level parameters.

This material is based upon work supported by the Office of Naval Research (ONR) under contract numbers N00014-23-C-1012, and N00014-24-C-1301. The views expressed are those of the author and do not reflect the official policy or position of the Department of War or the U.S. Government. DISTRIBUTION STATEMENT A. Approved for public release: distribution is unlimited. Approved 04/02/2026, DCN# 2026-3-19-2105.

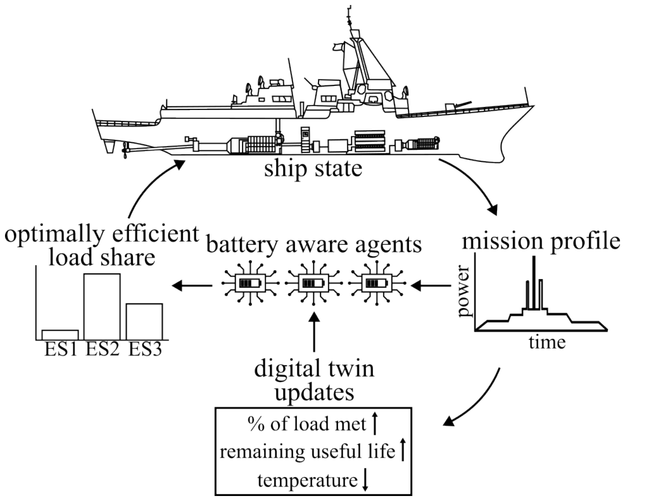

Fig. 1. Conceptual diagram of the adaptive agent-based control framework for a naval microgrid. "Ship state" and "mission profile" inputs inform "battery aware agents" that determine an optimal "load share" and adapt based on "digital twin updates" (e.g., RUL, SOC, temperature).

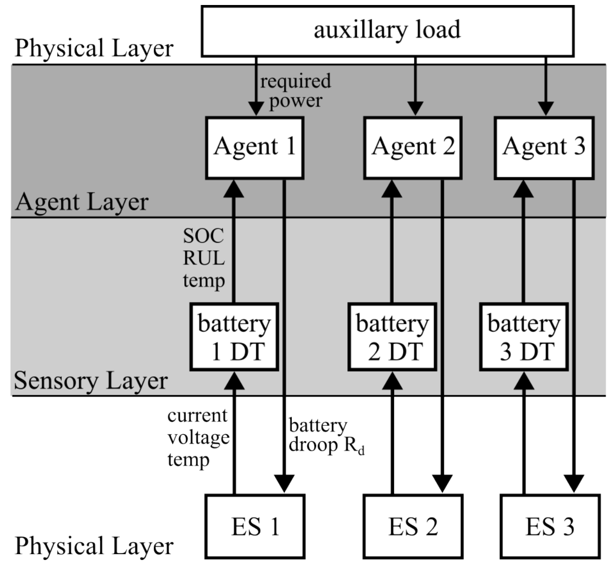

Fig. 2. The three-layer architecture of the adaptive agent framework when the auxillary load is active. The Physical Layer includes the ESS, bus, and load, the Sensory Layer uses digital twins to monitor state (SOC, RUL) in coordination with the Agent Layer to issue droop values (R_d) for each battery.

Inspired by this, a battery aware hierarchical droop method is proposed, allowing the agents decentralized control to account for system level battery states such as remaining-useful-life (RUL) and State of Charge (SOC) provided by the digital twin.

As shown in Fig. 1, to inform decision making and control logic, each adaptive agent receives local measurements and updates a battery digital twin. Each twin is used to model parameters unable to be directly observed by predicting temperature evolution, SOC, and RUL.

In this work, a new agent-based control strategy is explored using three distributed battery digital twins. The proposed adaptive agent-based control strategy targets power systems consisting of multiple ESS, and a variable load within a shared DC bus. Each agent dictates its corresponding ESS based on SOC, temperature, and health using a hierarchical droop scheme to allocate load share. This distributed control framework dynamically balances load support and storage utilization to meet mission-dependent load demands, reduce degradation, and improve overall resilience.

The contributions of this work are twofold. First, it details a control architecture for extending system life of a multi-battery DC microgrid, demonstrating an SOC and RUL informed hierarchical droop scheme. Second, it illustrates the use of adaptive agents in digital twins to ensure mission success and minimize system maintenance.

II. METHODOLOGY

A. Adaptive Agent-Based Control Framework

The adaptive agent-based control framework coordinates multiple distributed ESS, each comprising a battery, converter, and contactors, to satisfy bus demand while maintaining safe operating limits. An ESS is supervised through three layers: the physical layer, the sensory layer, and the agent layer, as shown in Fig. 2. The physical layer includes the battery hardware and converter control. The sensory layer contains the battery digital twin, which estimates state of charge, remaining useful life, and temperature from measured signals. The agent layer uses those estimates to select the operating mode and assign a droop coefficient.

The agent logic enforces constraints to maintain safe operation of its ESS. First, if the battery temperature exceeds a predefined maximum ($T_{\max}$), the agent sets the unit to idle, since charging or discharging at high temperature accelerates degradation leading to unstable behavior [9]. Otherwise, the agent selects an operating mode based on SOC and load activity:

1) if $SOC <= 10\%$, charge;
2) if $SOC >= 90\%$ and the auxiliary load is active, discharge;
3) if the pulse train has ended, charge;
4) otherwise (auxiliary load active and SOC within bounds), compute droop-based load sharing.

In droop mode, the converter output voltage is set by

$$V_{set,i} = V_{bus} - R_{d,i}\, I_i \tag{1}$$

where $V_{set,i}$ is the converter output voltage, V_{bus} is the auxiliary bus voltage, I_i is the ESS current contribution, and $R_{d,i}$ is the resistive droop coefficient. Using hierarchical droop, distributed agents manipulate $R_{d,i}$ at three levels. *Primary* control distributes load across all available ESS using a nominal droop resistance $R_{d,0} \approx 0.33$.

This was chosen to explore load sharing, assuming there are not constraints on bus voltage sag for this investigation.

Operating at the extremes of the SOC range accelerates degradation and heat generation in a lithium-ion battery [10],

[11]. Therefore, to encourage convergence toward mid-range SOC, *secondary* control influences the nominal droop resistance using

$$R_{d,\text{SOC}} = R_{d,\text{base}} \cdot (1 + \alpha(0.5 - SOC)\|0.5 - SOC\|) \quad (2)$$

where α is a constant that determines the rate that SOC will converge.

In implementation, $R_{d,i}$ must be bounded not only to avoid overly aggressive load sharing, but also to ensure the associated converter controls remain stable. Accordingly, the selected droop values are constrained to a stability-preserving range,

$$R_{d,\min} \leq R_{d,i} \leq R_{d,\max}, \quad (3)$$

where $R_{d,\min}$ is chosen to maintain adequate damping and phase margin of the combined inner current loop and outer voltage loop, and $R_{d,\max}$ is selected to limit steady-state bus-voltage deviation under the maximum expected current.

To prolong system life and decrease maintenance costs, the distributed ESS should reach end of life at approximately the same time t. The agent accomplishes this via the *tertiary* control using

$$R_{d,\text{RUL}} = \frac{R_{d,\text{SOC}}}{RUL^2} \quad (4)$$

where RUL is bounded by $RUL \in [0, 1]$.

RUL is defined from the capacity fade ratio C_i/C_0, where C_i is the current capacity and C_0 is the original capacity. The unit is considered end-of-life at 80% remaining capacity, so

$$RUL = 1 - \frac{1 - \frac{C_i}{C_0}}{0.2} \quad (5)$$

When charging, the agent uses a separate droop equation, to account for capacity fade during operation, given by

$$R_{d,\text{charge}} = \frac{1}{I_{\text{nom}}(1 - (\frac{1-RUL}{2}))} \quad (6)$$

where I_{nom} is the nominal charge current for the battery, determined by the manufacturer. However, this system is not designed to absorb surplus energy on the grid, so the contactors will open, rather than charge, when $SOC > 0.5$.

B. Digital twin implementation

Figure 3, shows the system architecture used to evaluate the proposed framework. The testbed consists of three ESS connected to a shared DC microgrid and tasked with supplying an auxiliary pulsed load. Each ESS contains a battery, a DC-DC converter, and contactors, and is supervised by a digital twin and an associated adaptive agent. The agent transmits a droop coefficient $R_{d,i}$ to the converter and receives measured voltage, current, temperature, and load-demand information. When the auxiliary load is inactive, the agent determines whether the battery should connect to the main bus for charging or remain in standby for thermal recovery.

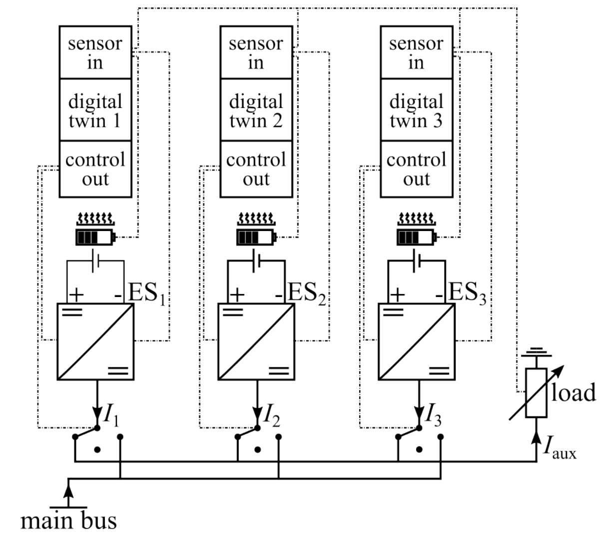

Fig. 3. Schematic of the experimental setup. A microgrid with three ESS ($\text{ES}_1, \text{ES}_2, \text{ES}_3$) is shown. Each ESS is governed by a digital twin running on a real-time controller to observe the system state, change voltage set points, and switch between charging, discharging, and standby.

To inform the adaptive agents, the digital twins must predict each battery SOC, RUL, and temperature, given the load profile. SOC estimation is done by coulomb counting as

$$SOC(i) = SOC_{i-1} - \frac{1}{C_i * 3600} \int (I(t)dt). \quad (7)$$

where C_i is the battery capacity in Ah, and I is the current at time step (t).

Proposed by Lam and Bauer, the event based capacity fade model dependent on temperature, state of charge, and depth of discharge for $LiFePO_4$ batteries is used [12]. By windowing data to the digital twin into 1800 s second frames, the capacity fade ξ_m during a window m, that discharges capacity Ah_m, is given as

$$\begin{aligned} &\xi(T_{avg}, SOC_{avg}, SOC_{dev}, Ah)_m \\ &= \Bigg(\Big(k_{s1} SOC_{dev,m} \cdot e^{(k_{s2} \cdot SOC_{avg,m})} \\ &+ k_{s3} e^{(k_{s4} \cdot SOC_{dev,m})} \Big) e^{\left(-\frac{E_a}{R}(\frac{1}{T_{avg,m}} - \frac{1}{T_{ref}})\right)} \Bigg) Ah_m \end{aligned} \quad (8)$$

where SOC_{avg} is the average SOC, and SOC_{dev} is the normalized deviation in SOC during window m given by

$$SOC_{dev} = \sqrt{\frac{3}{Ah_m} \int (SOC(i) - SOC_{avg})^2 dAh} \quad (9)$$

where Ah_m is the capacity discharged, or charged, within window m.

Lam and Bauer found the battery temperature to have an Arrhenius effect on degradation where E_a is the activation energy determined from testing, R is the gas constant, T_{avg}

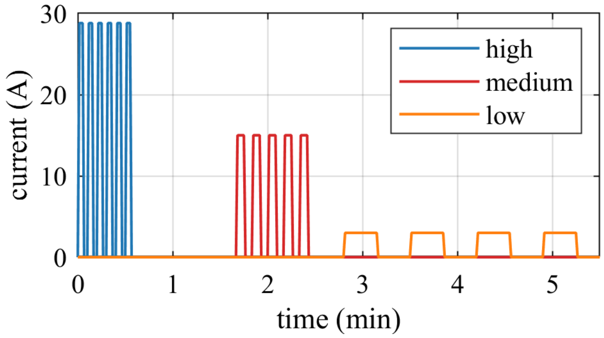

Fig. 4. The pulsed load sequence on the auxillary bus, recharging capacitors that power six 2 s, 28.8 A pulses, five 4 s, 15 A pulses, and four 20 s, 3 A pulses.

is the average temperature for window i, and T_{ref} is the reference temperature. Parameters denoted by $k_{s,i}$ are constants determined through curve fitting.

Before updating RUL to be employed in droop control, the active battery capacity C_i is then updated in the adaptive agent to equal C_m, the newly determined capacity, by

$$C_m = C_{m-1} - \xi_m \tag{10}$$

where $C_m - 1$ is the battery capacity estimated during the previous window.

Thermal behavior is captured by a lumped capacitance model describing the transient temperature $T(t)$ as

$$\begin{aligned} T(t) = T(t-1) + \Bigg[&-\frac{1}{C_{\text{lumped}} R_{\text{lumped}}} T(t-1) \\ &+ \frac{1}{C_{\text{lumped}} R_{\text{lumped}}} T_\infty + \frac{Q_{\text{gen}}}{C_{\text{lumped}}} \Bigg] \Delta t. \end{aligned} \tag{11}$$

where C_{lumped} and R_{lumped} are the effective thermal mass and resistance to ambient air or coolant.

The generated heat Q_{gen} combines ohmic and polarization losses with an entropic term that may be neglected at moderate C-rates, resulting in

$$\begin{aligned} Q_{\text{gen}} = I(t)[V_{\text{OCV}}(\text{SOC}, T) - V_{\text{term}}(t)] \\ + I(t) \frac{dV_{\text{OCV}}}{dT}. \end{aligned} \tag{12}$$

Moving from single-cell to pack level follows linear scaling, where current is divided by parallel cells and voltage is multiplied by cells in series.

III. Results

To evaluate the adaptive agent framework, each battery alternates between the main DC bus for charging and the auxiliary-load bus for pulsed-load support, as shown in figure 3. The test profile consists of high-rate, medium-rate, and low-rate pulse groups with total energies of 34.56 kJ, 30 kJ, and 24 kJ, respectively, as shown in figure 4. The auxillary load sequence is repeated until one ESS reaches end of life threshold, or $RUL = 0$.

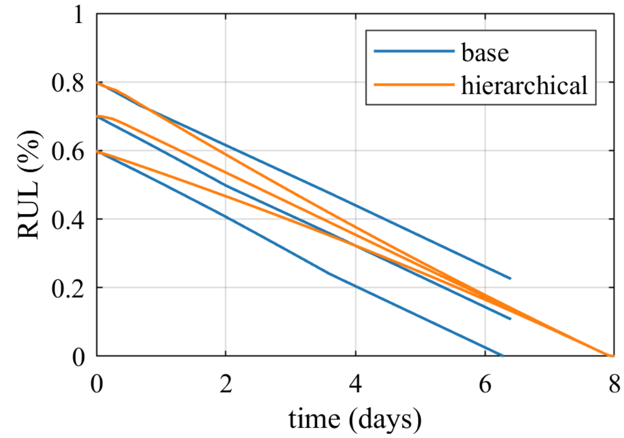

Fig. 5. The simulated RUL of each ESS with hierarchical and primary droop control. Primary droop evenly distributes the load, while hierarchical is both SOC and RUL aware.

In simulation, the agents with hierarchical control are tested when ES1, ES2, and ES3 begin at 80%, 70%, and 60% RUL, and 80%, 60%, and 40% SOC, respectively. Under primary droop with equal load sharing, the system lifetime is 6.4 days, as shown in Fig. 5. When compared to primary control, the adaptive agents, employing all three levels of hierarchical droop extends lifetime to 7.9 days, corresponding to a 23% longer system lifetime. To reduce simulation time, the capacity-degradation term was multiplied by 1000 at each step. Therefore, the reported lifetime values should be interpreted as relative comparison metrics rather than physical service-life predictions. If actually employed, the system would last $\approx$ 8000 days and over 1000 times as many cycles. Furthermore, the initial difference between the lowest and highest RUL is only 20%. When the system is run with a greater difference in RUL, the increase in lifetime expectation due to hierarchical droop becomes greater.

Figure 6 shows the current sharing and SOC of each battery under hierarchical droop control. Early in the test, SOC converges within 0.3 days, or 7.2 hrs, limited by the maximum discharge rate of 28.8 A per battery, before the load share begins to prioritize RUL. Furthermore, across battery lifetime, the auxiliary load requested is met for 100% of the test. Comparing RUL governed by hierarchical control in figure 5 to the load share in figure 6, the load distribution trajectory changes proportional to the RUL distribution between each ESS to increase system lifespan.

IV. Conclusion

Ensuring reliable power support in naval microgrids requires coordinated use of distributed battery resources while respecting electrical behavior and thermal limitations. By pairing an adaptive decentralized control approach with digital twin informed hierarchical droop, this work presents a method for balancing mission success against battery degradation. In simulation, hierarchical droop prolonged system operational lifetime by 23% relative to primary droop with equal load

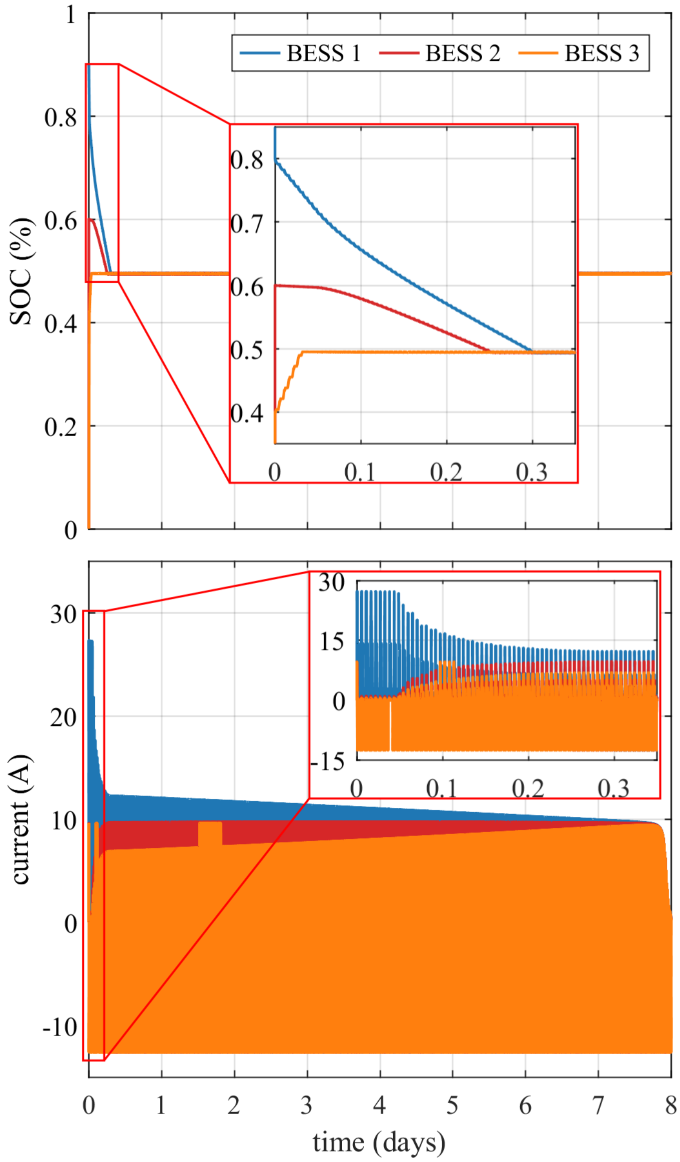

Fig. 6. The load share and SOC for each ESS with hierarchical droop control.

sharing. The adaptive-agent control also achieved SOC convergence in 7.2 h while meeting all pulsed loads on the auxiliary bus. The presented framework introduces a control approach that extends the operational life of a multi-battery DC microgrid and shows how digital twin informed agents can improve mission reliability and reduce maintenance burden.

Future work will integrate real-time hardware measurements with higher-fidelity battery twins to improve online state estimation and enable adaptive reconfiguration under changing thermal and degradation conditions.

V. Acknowledgment

This material is based upon work supported by the Office of Naval Research (ONR) under contract numbers N00014-23-C-1012, and N00014-24-C-1301. The views expressed are those of the author and do not reflect the official policy or position of the Department of War or the U.S. Government. DISTRIBUTION STATEMENT A. Approved for public release: distribution is unlimited. Approved 04/02/2026, DCN# 2026-3-19-2105.

References

[1] Y. Yuan, J. Wang, X. Yan, B. Shen, and T. Long, "A review of multi-energy hybrid power system for ships," *Renewable and Sustainable Energy Reviews*, vol. 132, p. 110081, 2020. [Online]. Available: https://www.sciencedirect.com/science/article/pii/S1364032120303725

[2] E. Crespo and A. Bazzi, "Mitigating directed energy pulsed load effects using distributed lithium-ion batteries and load control models," in *2025 IEEE Electric Ship Technologies Symposium (ESTS)*, 2025, pp. 275–282.

[3] Hanzaei et al., "Control of dc microgrids: A review," in *2021 31st Australasian Universities Power Engineering Conference (AUPEC)*, 2021, pp. 1–6.

[4] Díaz et al., "Centralized control architecture for coordination of distributed renewable generation and energy storage in islanded ac microgrids," *IEEE Transactions on Power Electronics*, vol. 32, no. 7, pp. 5202–5213, 2017.

[5] N. Altin, S. E. Eyimaya, and A. Nasiri, "Multi-agent-based controller for microgrids: An overview and case study," *Energies*, vol. 16, no. 5, 2023. [Online]. Available: https://www.mdpi.com/1996-1073/16/5/2445

[6] *Adaptive Agent-Based Control for Lithium-Ion Batteries in Naval Microgrids*, ser. International Design Engineering Technical Conferences and Computers and Information in Engineering Conference, vol. Volume 3A: 50th Design Automation Conference (DAC), 08 2024. [Online]. Available: https://doi.org/10.1115/DETC2024-143181

[7] L. Che and M. Shahidehpour, "Dc microgrids: Economic operation and enhancement of resilience by hierarchical control," *IEEE Transactions on Smart Grid*, vol. 5, no. 5, pp. 2517–2526, 2014.

[8] L. Meng, T. Dragicevic, J. C. Vasquez, and J. M. Guerrero, "Tertiary and secondary control levels for efficiency optimization and system damping in droop controlled dc–dc converters," *IEEE Transactions on Smart Grid*, vol. 6, no. 6, pp. 2615–2626, 2015.

[9] Peng et al., "Quantitative analysis of active lithium loss and degradation mechanism in temperature accelerated aging process of lithium-ion batteries," *Advanced Functional Materials*, vol. 34, no. 42, p. 2404495, 2024. [Online]. Available: https://advanced.onlinelibrary.wiley.com/doi/abs/10.1002/adfm.202404495

[10] Chowdhury et al., "Influence of state of charge window on the degradation of tesla lithium-ion battery cells," *Journal of Energy Storage*, vol. 76, p. 110001, 2024. [Online]. Available: https://www.sciencedirect.com/science/article/pii/S2352152X2303400X

[11] G. Liu, M. Ouyang, L. Lu, J. Li, and X. Han, "Analysis of the heat generation of lithium-ion battery during charging and discharging considering different influencing factors," *Journal of Thermal Analysis and Calorimetry*, vol. 116, no. 2, pp. 1001–1010, May 2014. [Online]. Available: https://doi.org/10.1007/s10973-013-3599-9

[12] L. Lam and P. Bauer, "Practical capacity fading model for li-ion battery cells in electric vehicles," *IEEE Transactions on Power Electronics*, vol. 28, no. 12, pp. 5910–5918, 2013.